

WINDS, B -FIELDS, AND MAGNETOTAILS OF PULSARS

M. M. ROMANOVA, G. A. CHULSKY, AND R. V. E. LOVELACE

Department of Astronomy, Cornell University, 412 Space Sciences Building, Ithaca, NY 14853

Received 2004 May 9; accepted 2005 May 6

ABSTRACT

We investigate the emission of rotating magnetized neutron stars due to the acceleration and radiation of particles in the relativistic wind and in the magnetotail of the star. We consider that the charged particles are accelerated by driven collisionless reconnection. Outside the light cylinder, the star's rotation acts to wind up the magnetic field to form a predominantly azimuthal, slowly decreasing with distance, magnetic field of opposite polarity on either side of the equatorial plane normal to the star's rotation axis. The magnetic field annihilates across the equatorial plane, with the magnetic energy going to accelerate the charged particles to relativistic energies. For a typical supersonically moving pulsar, the star's wind extends outward to the standoff distance with the interstellar medium. At larger distances, the power output of the pulsar's wind \dot{E}_w of the electromagnetic field and relativistic particles is *redirected and collimated into the magnetotail* of the star. In the magnetotail it is proposed that equipartition is reached between the magnetic energy and the relativistic particle energy. For such conditions, synchrotron radiation from the magnetotails may be a significant fraction of \dot{E}_w for high-velocity pulsars. An equation is derived for the radius of the magnetotail $r_m(z')$ as a function of distance z' from the star. For large distances z' , on the order of the distance traveled by the star, we argue that the magnetotail has a "trumpet" shape because of the slowing down of the magnetotail flow. We compare results with the Guitar Nebula and Mouse Nebula and conclude that the tail of the Mouse Nebula may be connected with the long magnetotail behind the pulsar. We argue that the shock waves and elongated structures may also be observed in misdirected or shutoff pulsars and may be used as a tool for finding these objects.

Subject headings: pulsars: general — stars: magnetic fields — stars: neutron — X-rays: stars

1. INTRODUCTION

The relativistic winds of supersonically moving pulsars are observed to form shock waves in the interstellar medium (ISM) and in some cases prominent wakes or "tails." Several pulsars are known to power bow shock waves and tails, such as the Guitar Nebula (Cordes et al. 1993; Chatterjee & Cordes 2002), millisecond pulsars (Kulkarni & Hester 1988; Bell et al. 1995), the Duck Nebula (e.g., Thorsett et al. 2002), the Mouse Nebula, observed in the X-ray and radio bands and powered by the spin-down of a 98 ms pulsar (Camilo et al. 2002; Gaensler et al. 2004), the pulsar B0740–28 (Jones et al. 2002), and the neutron star candidate RX J1856.5–3754 (van Kerkwijk & Kulkarni 2001a, 2001b). Axisymmetric simulations of the interaction of magnetized stars with the ISM have shown that such interaction leads to the formation of long magnetotails behind the stars (Romanova et al. 2001; Toropina et al. 2001). Such magnetotails may allow relativistic particles from the pulsar to propagate to large distances behind the pulsar.

In isolated pulsars a relativistic magnetohydrodynamic (MHD) wind forms outside the light cylinder and propagates outward (Goldreich & Julian 1969, hereafter GJ69; Arons & Tavani 1994; Arons 2004). This wind forms a magnetically dominated, azimuthally wrapped disk-like equatorial structure that expands with velocities on the order of the speed of light and is driven mostly by the magnetic pressure. Observations reveal disk-like structures around a number of pulsars, including one in the Crab Nebula (Weisskopf et al. 2000), the Vela pulsar (Pavlov et al. 2001), and a few other cases (Helfand et al. 2001; Gotthelf 2001). The orientation and thickness of these disk-like structures (or pulsar wind nebula [PWN] tori) were estimated by Ng & Romani (2004), who suggested that particles are accelerated more efficiently in these disk-like structures. It was also noticed

that the rotation axis of the disk approximately coincides with the direction of the pulsar's velocity, so that the geometry of the flow is approximately axisymmetric (Spruit & Phinney 1998; Lai et al. 2001). In a few cases jets were observed that are approximately aligned with the direction of motion (e.g., Weisskopf et al. 2000).

Formation of such an equatorial disk structure was recently modeled in axisymmetric relativistic MHD simulations by Del Zanna et al. (2004) and Komissarov & Lyubarsky (2004) for the case of an initial split monopole magnetic field. They have shown that a magnetically dominated disk is formed around a rotating pulsar and that this disk has a small thickness. Formation of rotating, azimuthally wrapped disk-like structures was also observed in nonrelativistic axisymmetric simulations of an accreting, rotating star with an aligned dipole magnetic field in the propeller regime (Romanova et al. 2003). This disk-like magnetically dominated bulk flow carries most of energy out of the pulsar; however, it may be invisible unless the particles are accelerated by some mechanism.

Different models have been proposed to explain the acceleration of particles in this wind. In one class of models *ideal* relativistic magnetohydrodynamics is assumed to hold outside the light cylinder with the acceleration of plasma due to the spatial variation of the electric and magnetic fields (e.g., Vlahakis 2004). In these models it is suggested that the Poynting flux-to-matter-energy flux ratio (σ) evolves from a value much larger than unity near the light cylinder to a value less than unity at large distances where the pulsar wind encounters the interstellar medium. In another class of models *nonideal* plasma effects are considered to be responsible for the particle acceleration. The particle acceleration may be stochastic, as discussed in the shock wave acceleration models (Arons & Tavani 1994; Arons 2004; Spitkovsky & Arons 2004b). Alternatively, in collisionless

reconnection and annihilation the magnetic field may cause random (Coroniti 1990) or bulk acceleration of the particles (Lyubarsky & Kirk 2001; Kirk & Lyubarsky 2001). These models argue that the MHD wind consists of an azimuthally wrapped dipole magnetic field of the star with regions where the magnetic field reverses direction. These regions are likely sites for reconnection and particle acceleration.

In this work we investigate a model in which particles are accelerated in the pulsar's *equatorial* neutral layer across which the predominantly azimuthal magnetic field reverses direction. There may also be oppositely directed Poynting flux flows aligned with the star's rotation axis analogous to those generated from the time-dependent expansion of magnetic field loops of an accretion disk into a low-density coronal plasma, as discussed by Lovelace & Romanova (2003) and simulated by Lovelace et al. (2005) with a relativistic electromagnetic particle-in-cell method. However, note that numerical solutions of the "pulsar equation" for an aligned stationary magnetosphere by Contopoulos et al. (1999) and Gruzinov (2005) do not show Poynting flows along the rotation axis.

Our model is qualitative in that we do not have global self-consistent calculations of the electromagnetic fields and sources. Compared to Coroniti (1990), we suppose that the misalignment angle between the rotational and magnetic axes is *not large*. Then instead of multiple neutral layers in a system of magnetic stripes, a global extended neutral layer forms in the equatorial plane. The equatorial layer is not expected to be thin everywhere. However, the systematic acceleration will be in the radial direction. Thus, the bulk motion of the plasma and magnetic field will be in the radial direction, mainly in the equatorial plane. Thus, we expect to have a high- σ plasma near the light cylinder that gradually changes to a much lower σ far from the pulsar. Accelerated particles will gradually diffuse vertically away from the thin neutral layer, and their interaction with the magnetic field will produce the synchrotron radiation. In this paper we develop this model in semiquantitative detail.

The acceleration of particles in collisionless reconnection has been discussed by a number of authors (Alfvén 1968; Dessler 1968, 1971; Speiser 1970; Cowley 1971, 1973; Bulanov & Sasorov 1976; Vasyliunas 1980; Burkhardt et al. 1991). The present work uses the model by Alfvén (1968) and its relativistic counterpart (Romanova & Lovelace 1992; Zenitani & Hoshino 2001; Larrabee et al. 2003). Both the simulations (Zenitani & Hoshino 2001) and the analytic theory (Larrabee et al. 2003) indicate a power-law distribution of accelerated particles.

Most pulsars propagate through the ISM highly supersonically so that the pulsar wind forms a strong shock wave in the ISM. A model of this interaction was first discussed by Schwartzman (1970). Subsequently, the shape of the shock wave was calculated for the hydrodynamic flow by Baranov et al. (1971), Baranov & Malama (1993), and Wilkin (1996). However, for the pulsar case it is necessary to include the relativistic magnetized wind of the star. Recent models of the solar wind interaction with the ISM include the influence of the magnetic field for both the interstellar and interplanetary components, and these models show that the shape of the bow shock may depend on these fields (e.g., Linde et al. 1998; Zank 1999; Opher et al. 2004). However, only relatively low Mach numbers are considered, and the Alfvén speeds are typically small compared with the flow speeds. In the case of pulsars, the Mach numbers are much larger than unity, and the Alfvén speeds may be comparable with the flow speeds. Strongly magnetized magnetotails were observed in axisymmetric simulations of rotating and nonrotating strongly magnetized stars (Toropina et al. 2001).

In this paper we discuss the nature of the magnetotails that form behind the pulsars. We argue that most of the power of the star's wind of relativistic particles and magnetic field is *redirected* by the internal shock wave and subsequently propagates down the magnetotail. In several cases, observations show cometary structures aligned with the direction of propagation of the pulsar (e.g., Stappers et al. 2003; Gaensler et al. 2003), which may be the result of the pulsar wind propagating down the magnetotail.

Both shocks and magnetotails may appear in the case of misdirected pulsars or longer period, shutoff pulsars. We discuss the possible nature of the isolated neutron star candidate RX J1856.5–3754, which has a shock wave.

In § 2 we discuss basic considerations. In § 3 we discuss particle acceleration due to reconnection in the equatorial neutral layer of the star and in § 4 the associated synchrotron radiation. In § 5 we discuss the bow shock wave and the related magnetotail and its synchrotron emission. In § 6 we discuss examples of pulsars with tails. In § 7 we consider the possibility of observing wind and magnetotail-emitting stars in the solar neighborhood. In § 8 we give the conclusions of this work.

2. BASIC CONSIDERATIONS

A pulsar's light cylinder radius is

$$r_L = \frac{c}{\omega_*} = \frac{Pc}{2\pi} \approx 4.8 \times 10^9 P \text{ cm}, \quad (1)$$

where P is the period in seconds. The pulsar spins down owing to the relativistic wind that flows outward beyond the light cylinder distance (GJ69). This wind consists of an electromagnetic field and relativistic particles and has a power output (GJ69)

$$\dot{E}_w \approx B_L^2 r_L^2 c = \frac{\mu^2 \omega_*^4}{c^3} \approx 5.8 \times 10^{31} \frac{\mu_{30}^2}{P^4} \text{ ergs s}^{-1}, \quad (2)$$

where $B_L \equiv \mu/r_L^3$ is the magnetic field strength at the light cylinder radius and $\mu_{30} = \mu/(10^{30} \text{ G cm}^3)$ is the star's magnetic moment. The star's surface magnetic field is $B = B_{12} 10^{12} \text{ G}$, with $B_{12} = \mu_{30}/R_6^3$, where $R_6 = R_*/10^6 \text{ cm}$ and R_* is the star's radius.

Assuming the pulsar wind is approximately isotropic, the pressure of the wind varies as $p_w = \dot{E}_w/(4\pi R^2 c)$ for distances $R > r_L$ from the star. For a pulsar moving supersonically through the ISM, the pressure of the pulsar wind $p_w(z)$ balances the ram pressure of the ISM $\rho_{\text{ISM}} v^2$ at the stagnation point at a distance z_{sh} in front of the pulsar. This is the location of the bow shock of the pulsar. That is, $p_w(z_{\text{sh}}) = \rho_{\text{ISM}} v^2$ so that (Schwartzman 1970; Baranov et al. 1971; Wilkin 1996)

$$z_{\text{sh}} = \frac{B_L r_L}{(4\pi \rho_{\text{ISM}} v^2)^{1/2}} \approx 10^{14} \frac{B_{12}}{n_{\text{ISM}}^{1/2} v_8 P^2} \text{ cm}, \quad (3)$$

where $\rho_{\text{ISM}}/m_p \approx n_{\text{ISM}}$ (in units of particles per cubic centimeter) is the number density of the ISM with m_p the proton mass, and $v_8 = v/10^8 \text{ cm s}^{-1}$. The lateral width of the bow shock is $\approx z_{\text{sh}}$. Thus, the power that goes into *thermal heating* of the shocked interstellar gas is

$$\dot{E}_{\text{sh}} \approx \frac{3}{16} \rho_{\text{ISM}} v^3 \pi z_{\text{sh}}^2 \approx 0.9 \times 10^{28} \frac{v_8 B_{12}^2}{P^4} \text{ ergs s}^{-1}, \quad (4)$$

where the factor of 3/16 assumes a specific heat ratio of 5/3. The power \dot{E}_{sh} is extracted from the kinetic energy of the

motion of the star through the ISM. The slowing of the star’s motion is, however, negligible. Notice that the ratio

$$\frac{\dot{E}_{sh}}{\dot{E}_w} \approx \frac{3}{64} \frac{v}{c} \approx 1.56 \times 10^{-4} v_8 \quad (5)$$

is much smaller than unity.

3. MAGNETIC RECONNECTION

Outside the light cylinder the pulsar’s magnetic field is predominantly azimuthal. If the magnetic moment of the star is perpendicular to its rotation axis, then the azimuthal magnetic field forms “stripes” of opposite polarity that move outward relativistically (e.g., Coroniti 1990; Lyubarsky & Kirk 2001). Particles may be gradually accelerated by reconnection of the oppositely directed fields (Coroniti 1990). Most of the power flow is thought to be in the form of a magnetically dominated wind. That is, the ratio of the magnetic energy density to the kinetic energy density of the particles, the σ -parameter, is much larger than unity. As the distance from the light cylinder increases, σ decreases.

We consider the case in which the angle between the magnetic and rotation axes is not very large. The nature of the envisioned driving mechanism is sketched in Figures 1 and 2. This work focuses on the equatorial region of the flow, but for completeness the figures show possible Poynting outflows along the $\pm z$ axes. The plasma behavior is *nonideal*; it is *not* described by ideal MHD. We use both cylindrical (r, ϕ, z) and spherical (R, θ, ϕ) nonrotating coordinates to describe the electromagnetic field and particle motion for $R > r_L$. The rotation of the star wraps the field around the rotation axis so that it is predominantly azimuthal, as shown in Figure 1. For the case assumed here, $\omega_* \cdot \mu > 0$ and the field lines are wound up clockwise for $z > 0$ and counterclockwise for $z < 0$. Consequently, there is a *neutral layer* in equatorial plane where the azimuthal magnetic field

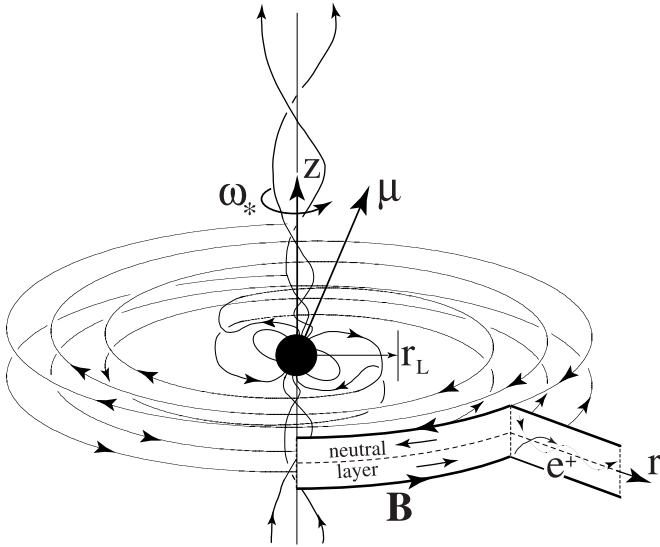


FIG. 1.—Sketch of the magnetic field configuration of a misaligned rotating neutron star outside the light cylinder, $r > r_L = c/\omega_*$. For the case shown, $\omega_* \cdot \mu > 0$, the magnetic field is wrapped in a clockwise spiral in the upper half-space and a counterclockwise spiral in the lower half-space. A neutral layer is formed in the equatorial plane where there is forced reconnection or annihilation of the magnetic field. The magnetic field energy goes into accelerating particles to relativistic energies. The helical field lines around the $\pm z$ axes correspond to possible Poynting outflows.

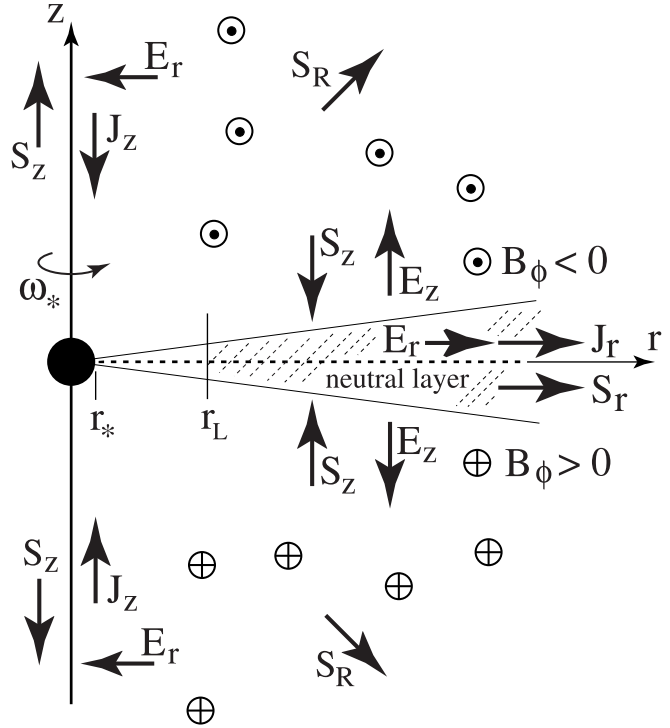


FIG. 2.—Current flows (J), electric fields (E), and Poynting vectors ($S = cE \times B/4\pi$) of the envisioned configuration outside the light cylinder, $r > r_L = c/\omega_*$.

changes from $B_\phi > 0$ for $z < 0$ to $B_\phi < 0$ for $z > 0$. Within the neutral layer, the magnetic field is approximated as

$$B_r = B_L \left(\frac{r_L}{r}\right)^2 \left(\frac{z}{\Delta z}\right), \quad B_\phi = -B_L \left(\frac{r_L}{r}\right) \left(\frac{z}{\Delta z}\right), \quad (6)$$

where $\Delta z(r)$ is the half-thickness of the neutral layer, which is assumed to be less than r , and $B_L \equiv \mu/r_L^3 \approx 9.2\mu_{30}/P^3$ G. Thus, the magnetic field has form of Archimedes’ spiral with field lines given by $r = \text{constant} - r_L\phi$. Equation (6) neglects the effect of the annihilation of the field.

In the neutral layer Ampère’s law gives $\partial B_\phi/\partial z = -4\pi J_r/c$. Thus, the change in the azimuthal field across the layer is

$$\Delta B_\phi = [B_\phi]_{-\Delta z}^{\Delta z} = -\frac{2I_r}{cr}. \quad (7)$$

Thus, the radial current carried by the neutral layer is

$$I_r = B_L r_L c \approx 4.4 \times 10^{11} \frac{\mu_{30}}{P^2} \text{ A}, \quad (8)$$

where $\mu_{30} \equiv \mu/(10^{30} \text{ G cm}^3)$ is the magnetic moment of the star. This radial equatorial current flow acts to *magnetically pinch* the particles within the neutral layer. An analogous current layer exists in the solar wind (e.g., Bertin & Coppi 1985).

The equatorial outflow of current is balanced by an axial inflow of current, as indicated in Figure 2. This current corresponds to a particle outflow rate of

$$\frac{dN}{dt} \approx \frac{I_r}{e} \approx 2.7 \times 10^{30} \frac{\mu_{30}}{P^2} \text{ s}^{-1}. \quad (9)$$

There may be oppositely directed Poynting flux outflows along the rotation axis with

$$S_z = \begin{cases} \frac{c}{4\pi} E_r B_\phi > 0 & \text{for } z > 0, \\ \frac{c}{4\pi} E_r B_\phi < 0 & \text{for } z < 0, \end{cases}$$

outward along the star's rotation axis. These outflows would be analogous to the Poynting outflows from accretion disks (Lovelace & Romanova 2003; Lovelace et al. 2005).

For the considered case $\omega_* \cdot \mu > 0$, the electric charge of the neutral layer is dominantly positive. Thus, the charge of the layer gives rise to an outward radial electric field $E_r > 0$ and an axial field $E_z > 0$ for $z > 0$ and $E_z < 0$ for $z < 0$, as shown in Figure 2. The electric field gives rise to an axial $\mathbf{E} \times \mathbf{B} = E_r B_\phi \hat{z}$ (< 0 for $z > 0$ and > 0 for $z < 0$) drift of the azimuthal field and associated plasma into the neutral layer. This constitutes the driving force for the reconnection.

Additionally, there is a radially outward $\mathbf{E} \times \mathbf{B} = -E_z B_\phi \hat{r}$ drift of the particles in the neutral layer. The $\mathbf{E} \times \mathbf{B}$ drifts are of course in the same direction as the Poynting vector $\mathbf{S} = (c/4\pi)\mathbf{E} \times \mathbf{B}$, which is shown in Figure 2.

Particles are accelerated in the electric field E_r , which decreases with the distance as $1/r$ or faster. This dependence is determined by the fact that the energy comes from the magnetic field, $\sim B_\phi$, which varies as $1/r$ (see eq. [6]). There is an additional factor in equation (6), $z/\Delta z$, which takes into account the fact that at larger distances the relative thickness of the neutral layer will likely increase due to instabilities and turbulence. The instabilities may be driven by the misalignment of the rotation ω_* and magnetic μ axes. This is expected to lead to a faster than $1/r$ decrease of the field with distance. In addition, part of the energy of the field will go to acceleration of particles, which will cause E_r to fall off more rapidly than $1/r$. Thus, we introduce a parameterized dependence of the electric field within the neutral layer in the form

$$E_r = \alpha_E B_L \left(\frac{r_L}{r} \right)^q, \quad (10)$$

where α_E is a dimensionless quantity assumed to be a constant less than unity and q is another constant that characterizes how fast this electric field decreases with the distance. The overall electrical neutrality of the equatorial and axial regions implies that $q > 1$. At the boundary of the neutral layer $E_z(r, \Delta z) \approx \alpha'_E B_L (r_L/r)$, where α'_E is another dimensionless quantity assumed to be appreciably less than unity.

Neglecting for the moment radiative energy losses, positively charged particles drifting into the neutral layer are accelerated in the direction $\hat{r} + (r_L/r)\hat{\phi}$, which is approximately radial for $r \gg r_L$. The radial acceleration gives

$$\frac{d}{dt}(mc^2\gamma) \approx c \frac{d}{dr}(mc^2\gamma) \approx q\alpha_E c B_L \left(\frac{r_L}{r} \right)^q, \quad (11)$$

where m is the particle rest mass and e is its charge (Alfvén 1968). The approximation involves assuming that the particles move outward with speed $\approx c$. Integrating equation (11) from $r = r_L$ to $r \gg r_L$, we find

$$\gamma = 1 + \frac{e B_L r_L}{m c^2} \frac{\alpha_E}{(q-1)} \quad (12)$$

for $r \gg r_L$ and q not close to unity. For the case of leptons,

$$\gamma \approx 2.6 \times 10^7 \left(\frac{\alpha_E}{q-1} \right) \left(\frac{\mu_{30}}{P^2} \right). \quad (13)$$

For protons and heavier ions the numerical factor is $\lesssim 1.4 \times 10^4$. A smaller number of negatively charged particles is accelerated back toward the pulsar.

The outward kinetic energy flux of the particles accelerated in the neutral layer is

$$\begin{aligned} \dot{E}_{\text{kin}} &= mc^2(\gamma - 1) \frac{dN}{dt} = (B_L^2 r_L^2 c) \frac{\alpha_E}{q-1} \\ &\approx 5.8 \times 10^{30} \left(\frac{\alpha_E}{0.1} \right) \frac{\mu_{30}^2}{P^4} \text{ ergs s}^{-1} \end{aligned} \quad (14)$$

for $r \gg r_L$, neglecting the synchrotron losses. This kinetic energy flux is a fraction $\alpha_E/(q-1)$ of the Goldreich-Julian power ($B_L^2 r_L^2 c$).

We expect different behaviors for the case in which q is appreciably larger than unity and the case in which q is close to unity. In the first case, particles are accelerated mainly in the vicinity of the light cylinder. In the second case, they are accelerated along the neutral layer out to much larger distances. The total energy, however, cannot be larger than the rotational energy of the pulsar; that is, $\alpha_E/(q-1) \leq 1$.

Particles, accelerated in the neutral layer, will be gradually scattered by irregularities (Alfvén waves) in the magnetic field and will drift away from the neutral layer. At the same time there may be magnetic confinement of particle to the neutral layer out to large distances. The force balance (or magnetic pinch) condition for the neutral layer follows from the momentum equation $\partial T_{zz}/\partial z = 0$ or $T_{zz} = \text{constant}$ (Bertin & Coppi 1985), where T_{jk} is the stress tensor for the particles and fields. This condition implies that $\alpha_E = (\Delta z/r)[1 - (\alpha'_E)^2]$. The compressive pinch force on the neutral layer is responsible for the reconnection at $z = 0$ being driven.

With increasing distance from the light cylinder, the ratio of the Poynting to particle energy fluxes, σ , decreases. The variation of σ with distance may be anisotropic, with smaller σ in the disk and larger σ above and below the disk. With increasing r , a larger fraction of the magnetic energy is converted to particle energy in the neutral layer. Particles accelerated in the neutral layer may subsequently scatter so as to give a more spherical wind. The scattering and diffusion processes of particles accelerated in the neutral layer remains to be investigated in detail. For simplicity of the following analysis, we suppose that $\sigma \lesssim 1$ before the bow shock is reached so that the flow is super-Alfvénic and supersonic at the bow shock.

4. SYNCHROTRON RADIATION

The acceleration of leptons in the neutral layer is inhibited due to the energy lost to synchrotron radiation. Including the synchrotron losses gives

$$\frac{d\gamma}{d\tilde{r}} = \frac{\gamma_0}{\tilde{r}^q} - \frac{k\gamma^2}{\tilde{r}^2}. \quad (15)$$

Here $\tilde{r} \equiv r/r_L$; $\gamma_0 \equiv e\alpha_E B_L r_L/(mc^2)$; $k \equiv \frac{2}{3}\beta_R B_L^2 r_L^2/(mc^2)$, with $r_e = e^2/(mc^2)$ the classical electron radius; and $\beta_R < 1$ accounts for the fact that the magnetic field close to the neutral layer is less than B_L/\tilde{r} . We assume that $\gamma \sim 1$ at the light cylinder distance $\tilde{r} = 1$. The synchrotron radiation of ions is negligible. Equation (15) represents a simplified model of the synchrotron losses from the neutral layer in that it neglects the fact that the leptons tend to be focused to the $z = 0$ plane, where the magnetic field is appreciably reduced. However, this focusing will be offset if, as expected, there are significant irregularities (turbulence) in the plasma and the magnetic field, as in the solar wind.

For simplicity we examine the case in which $q = 2$. It is clear that the Lorentz factors will not exceed

$$\begin{aligned}\gamma_{\max} &= \left(\frac{\gamma_0}{k}\right)^{1/2} = \left(\frac{3e\alpha_E r_L^3}{2\beta_R r_e^2 \mu}\right)^{1/2} \\ &\approx 3.1 \times 10^7 \left(\frac{\alpha_E}{\beta_R}\right)^{1/2} \frac{P^{3/2}}{\mu_{30}^{1/2}}.\end{aligned}\quad (16)$$

Thus, the synchrotron losses are significant for pulsar periods P shorter than the period that gives $\gamma_{\max} = \gamma_0$. This critical period is

$$P_{\text{cr}} = \frac{2\pi}{c} \left(\frac{2\alpha_E \beta_R r_e^3 \mu^3}{3emc^2}\right)^{1/7} \approx 0.49 \left(\frac{\alpha_E \beta_R}{0.01}\right)^{1/7} \mu_{30}^{3/7} \text{ s}.\quad (17)$$

For $P < P_{\text{cr}}$ the synchrotron energy-loss rate is

$$\begin{aligned}\dot{E}_{\text{syn}} &= \int_{r_L}^{\infty} dr I_r E_r = \alpha_E B_L^2 r_L^2 c \\ &\approx 5.8 \times 10^{30} \left(\frac{\alpha_E}{0.1}\right) \frac{\mu_{30}^2}{P^4} \text{ ergs s}^{-1},\end{aligned}\quad (18)$$

which is a fraction α_E of the Goldreich-Julian power. For $P < P_{\text{cr}}$ the kinetic energy flux of the particles is

$$\begin{aligned}\dot{E}_{\text{kin}} &= (\gamma_{\max} - 1)mc^2 \frac{dN}{dt} \\ &\approx 7 \times 10^{31} \left(\frac{\alpha_E}{\beta_R}\right)^{1/2} \frac{\mu_{30}^{1/2}}{P^{1/2}} \text{ ergs s}^{-1}.\end{aligned}\quad (19)$$

For $P < P_{\text{cr}}$ we have $\dot{E}_{\text{kin}}/\dot{E}_{\text{syn}} \approx 12.2(P^{7/2}/\mu_{30}^{3/2}) < 1$ for $\alpha_E = 0.1 = \beta_R$.

For $P > P_{\text{cr}}$ the synchrotron losses are small compared with power input to the particles in the neutral layer. The total synchrotron radiation from the neutral layer ($r \geq r_L$) is

$$\begin{aligned}\dot{E}_{\text{syn}} &= \frac{2}{3} r_e^2 r_L \beta_R B_L^2 \gamma_0^2 \frac{dN}{dt} \\ &\approx 3.9 \times 10^{29} \beta_R \left(\frac{\alpha_E}{0.1}\right)^2 \frac{\mu_{30}^5}{P^{11}} \text{ ergs s}^{-1}.\end{aligned}\quad (20)$$

The kinetic energy input to the particles in the neutral layer is $\alpha_E B_L^2 r_L^2 c$.

The synchrotron radiation of the particles accelerated in the neutral layer is beamed radially outward in the equatorial plane of the pulsar. That is, the radiation is in a fan beam perpendicular to the pulsar's rotation axis. In reality, the neutral layer is probably not a thin layer with small width Δz everywhere. The accelerated particles will scatter from irregularities in the neutral layer and interact with the magnetic field at larger distances, $z \gg \Delta z$. This process may explain the radiation from the disk-like PWNs such as those in the Crab Nebula and Vela Nebula.

For $P < P_{\text{cr}}$ the frequency of the peak of the radiation spectrum is

$$\begin{aligned}\nu_{\text{syn}} &\approx \frac{1}{4\pi} \frac{eB_L \gamma^2}{mc} \left(\frac{r_L}{r}\right) \\ &\approx 1.3 \times 10^{22} \left(\frac{\alpha_E}{\beta_R}\right) \left(\frac{r_L}{r}\right) \text{ Hz},\end{aligned}\quad (21)$$

where the lepton Lorentz factor is from equation (16). This frequency corresponds to a photon energy of ≈ 54 MeV. For $P > P_{\text{cr}}$, the Lorentz factor of the leptons is γ_0 so that

$$\nu_{\text{syn}} \approx 8.5 \times 10^{19} \left(\frac{\alpha_E}{0.1}\right)^2 \frac{\mu_{30}^3}{P^7} \text{ Hz}.\quad (22)$$

This frequency corresponds to ≈ 350 keV. These numbers are of course estimates because the value of α_E is not known.

5. THE MAGNETOTAIL

Beyond the light cylinder, the pulsar relativistic wind carries the power $\dot{E}_w = B_L^2 r_L^2 c$ in the electromagnetic field and relativistic particles (GJ69). The spin-down of the pulsar is given by $I\omega_* \dot{\omega}_* = -\dot{E}_w$, which implies that

$$P^2 = P_0^2 \left(1 + \frac{t}{\tau}\right), \quad \tau \equiv \frac{IP_0^2 c^3}{8\pi^2 \mu^2},\quad (23)$$

where t is the age of the pulsar, P_0 is the initial period of the pulsar, and $\tau \approx 1.4 \times 10^{11} (P_0/0.02 \text{ s})^2 / \mu_{30}^2 \text{ s} \approx 4300 (P_0/0.02 \text{ s})^2 / \mu_{30}^2 \text{ yr}$, assuming $I = 10^{45} \text{ g cm}^2$. After a time t the total energy put out by the pulsar is $E_w = I\omega_{*0}^2 [t/(t + \tau)]/2$, where $\omega_{*0} = 2\pi/P_0$.

The pulsar wind also carries toroidal magnetic flux outward. The rate of transport of positive toroidal flux is

$$\dot{\Phi}_+ = \pi B_L r_L c \approx 4.1 \times 10^{21} \frac{\mu_{30}}{P^2} \text{ G cm}^2 \text{ s}^{-1}.\quad (24)$$

After a time t the total (positive) toroidal flux put out by the pulsar is $\Phi_+ = (\pi\mu\omega_{*0}^2 \tau/c) \ln(1 + t/\tau) = (\pi/2)\mu l c^2 \ln(1 + t/\tau)$. Of course the net flux is zero.

For early times after the pulsar's birth there is a spherical Sedov-Taylor "bubble" of plasma of radius $\mathcal{R}(t) \propto t^a$ with $a < 1$. Here we consider *late times* in the sense that the pulsar has had time to move outside this bubble. That is, we consider $t > \mathcal{R}(t)/v$, where v is the pulsar's velocity. This corresponds to $t > (3 \times 10^9 \text{ s})(\mathcal{R}_{\text{pc}}/v_8)$, where \mathcal{R}_{pc} is the bubble radius in pc and $v_8 \equiv v/10^8 \text{ cm s}^{-1}$.

Figure 3 shows a sketch of the late stage of the magnetotail of a neutron star moving supersonically with velocity v through the interstellar medium. For simplicity we have assumed that the star's velocity is parallel to its rotation axis ω_* . The standoff distance of the shock z_{sh} is given by equation (3). The pulsar wind extends out to a radial distance $r_{m0} \approx z_{\text{sh}}$ from the z -axis at $z = 0$. The magnetic field strength at this distance is

$$\begin{aligned}B_{m0} &= B_L \left(\frac{r_L}{r_{m0}}\right) = (4\pi\rho_{\text{ISM}}v^2)^{1/2} \\ &\approx 4.6 \times 10^{-4} n_{\text{ISM}}^{1/2} v_8 \text{ G},\end{aligned}\quad (25)$$

which is independent of the period and magnetic moment of the pulsar. The magnetic field pressure of the wind at r_{m0} is

$$p_{m0} = \frac{B^2}{4\pi} \Big|_{r_{m0}} = \Gamma p_{\text{ISM}} M^2,\quad (26)$$

where p_{ISM} is the ambient pressure of the interstellar medium, Γ is the ratio of specific heats, and $M = v/c_s$ is the Mach number of the pulsar. Typically, $M \gg 1$, so that electromagnetic pressure at r_w is much larger than p_{ISM} . The pressure of the shocked interstellar gas is larger than p_{ISM} by a factor M^2 , neglecting

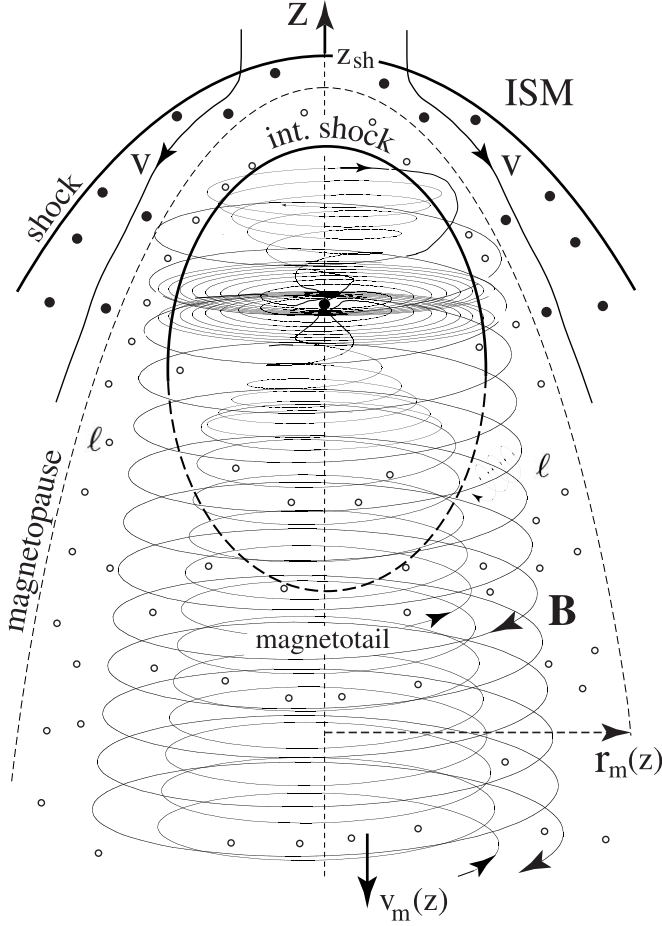


FIG. 3.—Sketch of the external shock, the magnetopause, and the magnetotail of a pulsar moving supersonically through the ISM. The velocity of the star is assumed parallel to the star's rotation axis ω_s . The filled circles indicate the shocked interstellar gas with sample streamlines labeled v . The open circles indicate relativistic leptons (l) that flow into the magnetotail. The radius of the magnetotail is $r_m(z)$, and the bulk velocity of the magnetotail plasma is $v_m(z)$. The internal shock of the pulsar wind is indicated by "int. shock." The standoff distance of the shock, z_{sh} , is given by eq. (3).

radiative cooling. Because the timescale $t_m \equiv r_{m0}/v$ is much shorter than the spin-down timescale τ , the time dependence of the pulsar's period can be neglected.

The momentum of the relativistic pulsar wind is *deflected* by the *internal shock*, as indicated in Figure 3. The flow of power and magnetic flux is, however, essentially unchanged. We assume that the internal shock has the effect of establishing an *approximate equipartition* between the field energy density and the energy density of the relativistic particles. It is unlikely that the pulsar's magnetized wind is compressed into a thin layer in contact with the interstellar medium, as discussed in the hydrodynamic model (Baranov et al. 1971; Wilkin 1996). Plasma in the magnetotail moves away from the pulsar with an initially *relativistic* velocity, $\mathbf{v}_m \approx v_{mz} \hat{z}$, where $v_{mz}(z=0) = O(c)$. As indicated in Figure 3, the magnetic field in the magnetotail is predominantly toroidal, $\mathbf{B} \approx \hat{\phi} B_m(z)$.

Inside the magnetotail there is a cylindrical neutral layer across which the magnetic field reverses direction (see also simulations by Romanova et al. [2001] and Toropina et al. [2001]). Reconnection or annihilation of the magnetic field in this layer continually accelerates the charged particles of the flow. In the following equations, we assume that the charged particles consist of electrons and positrons. The flux of particles from the pulsar is

$dN_l/dt \approx 2B_L r_L c/e$. In a steady state this particle flux flows down the magnetotail so that $dN_l/dt = \pi r_m^2 n_l v_{mz}$, where n_l is the lepton density. The equipartition Lorentz factor of the leptons is

$$\langle \gamma_l \rangle = \frac{1}{8} \frac{e B_L r_L}{m c^2} \left(\frac{B_m r_m}{B_{m0} r_{m0}} \right)^2 \frac{v_{mz}}{c} \approx 10^6 \frac{\mu_{30}}{P^2} \left(\frac{B_m r_m}{B_{m0} r_{m0}} \right)^2 \left(\frac{v_{mz}}{10^{10} \text{ cm s}^{-1}} \right), \quad (27)$$

where we have used the fact that $B_{m0} r_{m0} = B_L r_L$.

The total, kinetic plus field, energy flux along the magnetotail is

$$\mathcal{F}_E(z) = \frac{1}{2} (B_m r_m)^2 v_{mz}. \quad (28)$$

Assuming a *stationary* flow with respect to the pulsar, the synchrotron losses along the magnetotail imply

$$\frac{d\mathcal{F}_E}{dz'} = -(\pi r_m^2 n_l) \frac{2}{3} r_e^2 c B_m^2 \langle \gamma_l^2 \rangle,$$

or

$$\frac{d(\chi^2 v_{mz})}{dz'} = -\frac{1}{z_0} \left(\frac{r_{m0}}{r_m} \right)^2 \chi^6 v_{mz}, \quad (29)$$

where $z' \equiv -z \geq 0$ and

$$\chi \equiv \left(\frac{B_m}{B_{m0}} \right) \left(\frac{r_m}{r_{m0}} \right) \leq 1.$$

Here z_0 is the *radiation length-scale* of the magnetotail,

$$z_0 = \frac{24 m^2 c^4}{B_L r_L r_e^2 e (4\pi \rho_{ISM} v^2) C_l} \approx 15 \frac{P^2}{\mu_{30} n_{ISM} v_8^2 C_l} \text{ pc}, \quad (30)$$

and $C_l \equiv \langle \gamma_l^2 \rangle / \langle \gamma_l \rangle^2$ is a constant of order unity. Solutions of equation (29) for $v_{mz} = \text{constant}$ indicate that χ decreases very gradually with z' .

The frequency of the peak of the synchrotron radiation from the magnetotail is

$$\nu_{\text{syn}} \approx \frac{1}{4\pi} \frac{e B_m \gamma^2}{m c} \approx 7.4 \times 10^{14} \frac{\mu_{30}^2 n_{ISM}^{1/2} v_8}{P^4} \chi^5 \left(\frac{r_{m0}}{r_m} \right) \left(\frac{v_{mz}}{10^{10} \text{ cm s}^{-1}} \right)^2 \text{ Hz}, \quad (31)$$

where we have used equation (27) for the lepton Lorentz factor.

Most pulsar velocities through the ISM are less than 10^3 km s^{-1} , with typical velocities $\sim 100\text{--}500 \text{ km s}^{-1}$ (Arzoumanian et al. 2002). For these slower pulsars, the length z_0 may be larger than the total distance the pulsar has traveled. For such conditions only a small fraction of the magnetotail energy flux \mathcal{F}_E is lost to synchrotron radiation. Here we discuss the long-distance $z' \gg r_{m0}$ behavior of the magnetotail in this limit. The internal pressure of the magnetotail, p_m , is much larger than the pressure of the ISM at distance z' , $p_{ISM} = \rho_{ISM} c_s^2 / \Gamma \ll p_m$. In general, the radius of the magnetotail increases with distance from the

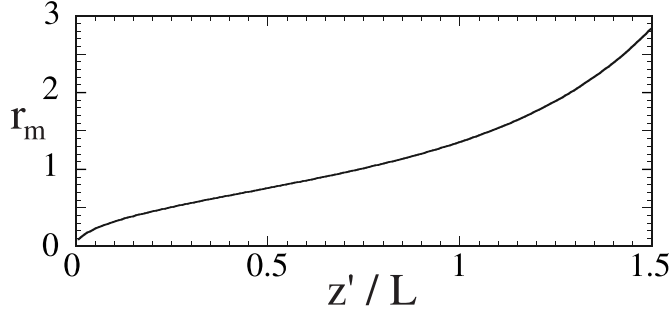


FIG. 4.—Qualitative dependence of the width of the magnetotail $r_m(z')$ on the distance behind the star z' . The vertical scale is arbitrary and is given by $(z'/L)^{1/2}F(z'/L)$, with F given below eq. (35).

star. Assuming a stationary configuration in the reference frame moving with the star, we have

$$\frac{dr_m(z')}{dz'} = \frac{v_{mr}}{v_{mz}},$$

$$v_{mr} = \left[\frac{p_m(z')}{\rho_{\text{ISM}}} \right]^{1/2} = \left(\frac{\dot{E}_w}{3\pi r_m^2 v_{mz} \rho_{\text{ISM}}} \right)^{1/2}. \quad (32)$$

Thus,

$$\frac{dr_m(z')}{dz'} = \left(\frac{4c}{3v_{mz}} \right)^{1/2} \frac{r_{m0}}{r_m} \frac{v}{v_{mz}}$$

$$\approx 0.02v_8 \left(\frac{r_{m0}}{r_m} \right) \left(\frac{10^{10} \text{ cm s}^{-1}}{v_{mz}} \right)^{3/2}. \quad (33)$$

Expressed in this form, dr_m/dz' is independent of \dot{E}_w and ρ_{ISM} . Equation (32) represents a balance of the internal pressure of the magnetotail, $p_m(z')$, against the ram pressure due to the tail's expansion into the ISM, $\rho_{\text{ISM}}(dr_m/dt)^2$, where $dz'/dt = v_{mz}$.

For distances $z' \gg r_{m0}$ but small compared with the total distance the star has traveled, v_{mz} is approximately constant. Consequently,

$$r_m(z') \approx 0.2(r_{m0}z')^{1/2} \left(\frac{10^{10} \text{ cm s}^{-1}}{v_{mz}} \right)^{3/4}, \quad (34)$$

for $z' \gg r_{m0}$.

The situation is different for distances z' on the order of or somewhat larger than the total distance traveled by the star, $L \equiv vt \approx 10v_8(t/10^4 \text{ yr}) \text{ pc}$, with t the age of the star. The velocity of the magnetotail plasma v_{mz} must decrease strongly with z' on the order of this distance because of collisions with the plasma of the above-mentioned bubble $\mathcal{R}(t)$ formed at the birth of the pulsar. For a rough description, consider

$$v_m(z') = v_m(0) \exp \left[-\frac{(z')^2}{L^2} \right].$$

For this case equation (33) gives

$$r_m(z') = 0.2(r_{m0}z')^{1/2} \left[\frac{10^{10} \text{ cm s}^{-1}}{v_{mz}(0)} \right]^{3/4} F \left(\frac{z'}{L} \right), \quad (35)$$

where

$$F(\xi) \equiv \left[\frac{1}{\xi} \int_0^\xi d\xi \exp \left(\frac{3\xi^2}{2} \right) \right]^{1/2}.$$

Figure 4 shows the qualitative dependence of $r_m(z')$. Notice that the curvature of the magnetotail radius d^2r_m/dz'^2 is initially negative, but at large $z' \gtrsim 0.45L$ it becomes positive. Further note that $v_{mz}(z')[r_m(z')]^2$ is an increasing function so that $B_m(z')$ decreases with distance from the star.

The magnetotails may be observable as low surface brightness regions of nonthermal, polarized (synchrotron) emission.

6. EXAMPLES OF MAGNETOTALS: GUITAR NEBULA AND MOUSE NEBULA

The Guitar Nebula is created by the high-velocity pulsar B2224+65. Chatterjee & Cordes (2002, 2004) estimate the velocity of the pulsar as $v_8 \approx 1.7$ or 1700 km s⁻¹ based on a distance to the source of $D = 1.9$ kpc. The pulsar period $P = 0.68$ s and spin-down rate $\dot{P} = 9.7 \times 10^{-15}$ s s⁻¹ imply a power output of $\dot{E} \approx 1.2 \times 10^{33}$ ergs s⁻¹, assuming a moment of inertia $I = 10^{45}$ g cm². The angular length of the tail is $\delta\theta \approx 15''$ (Chatterjee & Cordes 2004), which corresponds to a tail length $z' \approx (0.15 \text{ pc})/\sin \iota$, where ι is the angle between the jet axis and the line of sight. With $\dot{E} = B_L^2 r_L^2 c$, this power implies $\mu_{30} \approx 2.1$. Consequently, equation (30) gives the length-scale of the magnetotail $z_0 \approx (1 \text{ pc})/(n_{\text{ISM}} C_l)$. This corresponds approximately to the whole length of the tail in the Guitar Nebula observed in the H α line. Equation (31) gives the estimate $\nu_{\text{syn}} \approx (2.6 \times 10^{16} \text{ Hz}) n_{\text{ISM}}^{1/2} \chi^5 (r_{m0}/r_m) [v_{mz}/(10^{10} \text{ cm s}^{-1})]^2$. The Guitar Nebula was observed as a source of very weak radiation in soft X-rays, which is a sign of the presence of highly relativistic leptons, $\gamma \sim 10^7$ (Romani et al. 1997). Equation (13) gives similar γ for the Guitar Nebula. Both the magnetic field and the particles interact with the interstellar medium and are deflected to the tail. The radio images of the Guitar Nebula show clear limb brightening (e.g., Chatterjee & Cordes 2004). This may be due to the compression of the magnetic field at the shock wave, which leads to higher intensity of radiation (e.g., Romani et al. 1997). From the other side, enhanced reconnection is expected near the shock wave due to compression of the magnetic field components of opposite polarity. This will also lead to limb brightening. The inner (smaller scale) structure of the Guitar Nebula is closed in the back and may represent the inner shock wave, where accelerated particles were stopped by the interstellar medium. If this is the case, then the flow has $\sigma < 1$ before the shock wave.

Another example is the Mouse Nebula, which is created by the much more powerful pulsar PSR J1747–2958, which propagates with high velocity, $v \approx 600$ km s⁻¹ (Camilo et al. 2002). It has a period $P = 0.098$ s and a spin-down luminosity $\dot{E} \approx 2.5 \times 10^{36}$ ergs s⁻¹, which corresponds to $\mu_{30} \approx 2.5$. This extended radio nebula was discovered around this pulsar (Yusef-Zadeh & Bally 1987). An interesting feature is the tail, which propagates to very far distances. Recently, an X-ray nebula was found in observations with the *Chandra X-Ray Observatory* (Gaensler et al. 2004). Gaensler et al. (2004) estimate the X-ray luminosity of the nebula as $L_X(0.5–8 \text{ keV}) \approx 5 \times 10^{34}$ ergs s⁻¹, based on a distance to the source of $D = 5$ kpc, and the angular length of the Mouse Nebula tail as $\delta\theta \approx 45''$, which corresponds to a tail length $z' \approx (1 \text{ pc})/\sin \iota$. For these parameters and assuming $v_8 = 0.6$ and $n_{\text{ISM}} = 0.3 \text{ cm}^{-3}$ (Gaensler et al. 2004), equation (30) gives a radiation length-scale of the magnetotail of $z_0 \approx (0.5 \text{ pc})/C_l$. For this object equation (31) gives the estimate $\nu_{\text{syn}} \approx (2.7 \times 10^{19} \text{ Hz}) n_{\text{ISM}}^{1/2} \chi^5 (r_{m0}/r_m) [v_{mz}/(10^{10} \text{ cm s}^{-1})]^2$. The predicted frequency and overall luminosity is much higher than those for Guitar Nebula, which correspond to observations of a much brighter X-ray source.

The shape of the Mouse Nebula was modeled by hydrodynamic simulations (Gaensler et al. 2004; van der Swaluw et al. 2003; Bucciantini 2002). It was suggested that the inner brightest region of the nebula may be due to the termination shock of the pulsar wind, while the long tail may represent the postshock flow. We note that the *Chandra* observations do not show evidence of the shock wave in the X-ray picture of this nebula. Instead, the X-ray luminosity in the brightest region (the head of the Mouse Nebula) varies gradually (Gaensler et al. 2004). This may be a sign that in the tail the σ -parameter is not small and the backflow is not super-Alfvénic. If $\sigma \sim 1$ in the tail, then the magnetotail may propagate to very far distances (see, e.g., simulations by Romanova et al. [2001] and Toropina et al. [2001]). Radio radiation is then connected with particles that propagate from the pulsar along the tail to far distances and lose their energy there, or particles may be accelerated in situ during the reconnection processes in the magnetotail (Toropina et al. 2001).

The direction of jets observed in a few cases is almost aligned with the direction of propagation of the pulsar and seems to be perpendicular to the PWN disk (e.g., Ng & Romani 2004). If the direction of the pulsar's motion is determined by a magnetic kick during its formation (Ardeljan et al. 2001; Lai et al. 2001) then both ω_* and μ will be in the same direction. If the magnetic axis is misaligned relative to the rotational axis, but ω_* is aligned with the pulsar's velocity v , then the situation is similar to that described above, because the jet forms in the direction of ω_* and the disk magnetic structure is perpendicular to ω_* . However, if ω_* does not coincide with v , then both the jet and the PWN disk may give nonaxisymmetric features of the PWN. This latter situation has not been investigated. A related situation appears in the recently discovered double pulsar binary PSR J0737–3039 for which the direction of the flow from the wind-generating pulsar changes in time because of the motion of stars in the binary system (Kaspi et al. 2004; Demorest et al. 2004). Three-dimensional simulations of such a flow have shown that for large inclination angles between the magnetic and rotational axes of the pulsar, the shock wave may be nonaxisymmetric (Spitkovsky & Arons 2004a).

7. OBSERVABILITY OF WIND- AND MAGNETOTAIL-EMITTING STARS IN THE SOLAR NEIGHBORHOOD

Although neutron stars that spin down to periods $P \gtrsim 1\text{--}3$ s shut off as pulsars, they may continue to emit a wind and interact with the ISM. The number of such objects is larger than the number of short-period pulsars. It is possible that such objects are detectable at distances $\lesssim 10^2$ pc. The interesting nearby isolated neutron star candidate RX J1856.5–3754 has a prominent shock wave, and we discuss this object below.

Different spin-down powers \dot{E}_w are expected, depending on the star's period of rotation and magnetic field. We consider two cases, one with a relatively high spin-down power $\dot{E}_w \sim 10^{31}\text{--}10^{32}$ ergs s $^{-1}$, which is pertinent to old pulsars or relatively powerful shutoff pulsars, and one with a low spin-down power, $\dot{E}_w = 10^{28}$ ergs s $^{-1}$, corresponding to very weak shutoff pulsars.

7.1. Relatively High Spin-Down Power Objects

Shutoff or misdirected pulsars with periods $P \sim 1$ s and a surface magnetic field $B \sim 10^{12}$ G have a relatively high spin-down power, $\dot{E}_w \sim 6 \times 10^{31}$ ergs s $^{-1}$ (i.e., eq. [2]). The synchrotron emission from the pulsar wind for distances within the bow shock wave is given by equation (20), and the photon energies are given by equation (22) and are in the high X-ray range. Additionally, there will be a small power in thermal radiation from the shocked ISM according to equation (5). For high-velocity pulsars, say

$v > 500$ km s $^{-1}$, a significant fraction of the spin-down power is emitted in the magnetotail. The photon energies are then much lower, in the UV band according to equation (31). Such shutoff or misdirected pulsars could be observed because of the radiation of their tails.

7.2. Nature of RX J1856.5–3754

The source RX J1856.5–3754 is an interesting isolated neutron star candidate located at a distance $d \approx 60$ pc (Walter 2001). It has a bow shock wave observed by van Kerkwijk & Kulkarni (2001a, 2001b) in the H α line. The observed standoff distance between the star and the bow shock wave is $\approx 1''$, which corresponds to $z_{\text{sh}} \approx 0.9 \times 10^{15}$ cm. The bow shock is probably due to the interaction of the star's wind with the ISM (see, e.g., van Kerkwijk & Kulkarni 2001b). In this case we obtain from equation (3) the relation $B_{12}/(n_{\text{ISM}}^{1/2} v_8 P^2) \approx 9$, where B_{12} may be replaced by μ_{30} . This relation implies that the spin-down power of the star is $\dot{E}_w \approx 5.2 \times 10^{32} n_{\text{ISM}} v_8^2 \approx 5.2 \times 10^{30}$ ergs s $^{-1}$, where we took $v_8 = 0.1$ and $n_{\text{ISM}} = 1$ cm $^{-3}$.

Clearly, a range of values of B_{12} (or μ_{30}), P , and v_8 can give $\mu_{30}/(v_8 P^2) \approx 9$, where we have taken for simplicity $n_{\text{ISM}} = 1$ cm $^{-3}$. To consider the likely values, note that the spin-down time of the star is $t_{\text{sd}} \equiv P/\dot{P} = IP^2 c^3 / (4\pi^2 \mu^2) \approx (2.2 \times 10^7 \text{ yr}) P^2 / \mu_{30}^2$, assuming $I = 10^{45}$ g cm 2 . The total number of neutron stars likely to be within a distance of 60 pc of the Sun is $N \approx 10^9 [(60 \text{ pc}) / (10^4 \text{ pc})]^3 \approx 220$ (e.g., Schvartzman 1971; Treves & Colpi 1991). Then the probable number of objects with spin-down time t_{sd} within 60 pc is $N' \approx 220(t_{\text{sd}}/t_H)$, where $t_H \approx 1.5 \times 10^{10}$ yr is the Hubble time. Thus, for the object RX J1856.5–3754, $N' \approx 0.036/(\mu_{30} v_8)$. The corresponding rotation period of the star is $P \approx 0.33(\mu_{30}/v_8)^{1/2}$ s. Clearly, larger values of N' occur for smaller values of the product $\mu_{30} v_8$. For example, for $\mu_{30} = 0.1$ and $v_8 = 0.1$, $N' \approx 3.6$. For these values $\dot{E}_w \approx 5.2 \times 10^{30}$ ergs s $^{-1}$. So, this object may be a misdirected pulsar if the magnetic field is large or a shutoff pulsar if the field is small.

7.3. Low Spin-Down Power Objects

There should be a much larger number of shutoff pulsars with lower spin-down power. As an example, we take objects with the spin-down power $\dot{E}_w = 10^{28}$ ergs s $^{-1}$. For these objects, $\mu_{30}^2/P^4 \approx 1.7 \times 10^{-4}$, so that $P \approx 8.7 \mu_{30}^{1/2}$ s. The number of such objects within a distance of 60 pc of the Sun is $N' \approx 220(t_{\text{sd}}/t_H) \approx 24/\mu_{30}$. The standoff distance of the bow shock wave is, however, small, $z_{\text{sh}} \approx 1.3 \times 10^{12} v_8^{-1}$ cm, but much larger than the light cylinder radius.

8. DISCUSSIONS AND CONCLUSIONS

This work considers rotating magnetized neutron stars emitting power \dot{E}_w in a wind of relativistic particles and electromagnetic field. We argue that a nonnegligible fraction of the wind's power may be converted to relativistic particles due to annihilation or reconnection of the magnetic field. Outside the light cylinder, the star's rotation acts to wind up the magnetic field to form a predominantly azimuthal magnetic field of opposite polarity on either side of the equatorial plane normal to the star's rotation axis that slowly decreases with distance. An analogous situation exists in the solar wind (Bertin & Coppi 1985). The magnetic field annihilates across the equatorial plane with the magnetic energy accelerating the charged particles to highly relativistic energies. The accelerated leptons emit synchrotron radiation in a broad range from the UV to gamma-ray energies. Additionally, there may be oppositely directed Poynting outflows

along the star's rotation axis. These outflows are analogous to the Poynting jets discussed by Lovelace & Romanova (2003). The model is qualitative in the respect that we do not have global self-consistent calculations of the electromagnetic fields and sources.

For a typical supersonically moving star, the star's relativistic wind forms a bow shock wave with the interstellar medium (Schvartsman 1970). We argue that an appreciable fraction of the star's wind power \dot{E}_w is deflected by the bow shock wave and collimated into the star's magnetotail. Plasma moves down the magnetotail with a relativistic velocity. Furthermore, we argue that equipartition is reached in the magnetotail between the magnetic energy and the relativistic particle energy. For the case in which the charged particles are leptons, the synchrotron radiation length-scale z_0 of the magnetotail is calculated. Over this distance the energy flux in the magnetotail decreases by a factor of order 2. For highly supersonic pulsars, z_0 may be less than the total distance the star has traveled. The synchrotron radiation spectrum is expected to be nonthermal, with typical photon energies in the UV range for the highly supersonic pulsar B2224+65, which generates a bow shock wave, and the Guitar Nebula (Chatterjee & Cordes 2002).

The ratio of the power due to the shock heating of the ISM, which gives thermal emission, to the wind power \dot{E}_w , which gives nonthermal synchrotron emission, is shown to be $(3/64)(v/c) \ll 1$, where v is the velocity of the star and c is the speed of light.

An equation is derived for the radius of the magnetotail $r_m(z')$ as a function of distance z' from the star. For large distances z' , on the order of the distance traveled by the star, we argue that the magnetotail has a "trumpet" shape owing to the slowing down of the magnetotail flow.

We argue that the isolated neutron star candidate RX J1856.5–3754 may be a misdirected or shutoff pulsar.

We estimate the number of shutoff pulsars that may be observable in the vicinity of the Sun for cases of relatively strong (10^{32} ergs s⁻¹) and weak (10^{28} ergs s⁻¹) power. A much larger number of weak shutoff pulsars is predicted.

We thank Kaya Mori, David Chernoff, Jim Cordes, and George Pavlov for stimulating discussions. We thank an anonymous referee for thoughtful comments. This work was supported in part by NASA grants NAG5-13060 and NAG5-13220 and NSF grant AST 03-07817.

REFERENCES

- Alfvén, H. 1968, *J. Geophys. Res.*, 73, 4379
- Ardeljan, N. V., Bisnovatyi-Kogan, G. S., & Moiseenko, S. G. 2001, *Ap&SS Suppl.*, 276, 295
- Arons, J. 2004, *Adv. Space Res.*, 33, 466
- Arons, J., & Tavani, M. 1994, *ApJS*, 90, 797
- Arzoumanian, Z., Chernoff, D. F., & Cordes, J. M. 2002, *ApJ*, 568, 289
- Baranov, V. B., Krasnobaev, K. V., & Kulikovskii, A. G. 1971, *Soviet Phys.–Dokl.*, 15, 791
- Baranov, V. B., & Malama, Yu. G. 1993, *J. Geophys. Res.*, 98, 15157
- Bell, J. F., Bailes, M., Manchester, R. N., Weisberg, J. M., & Lyne, A. G. 1995, *ApJ*, 440, L81
- Bertin, G., & Coppi, B. 1985, *ApJ*, 298, 387
- Bucciantini, N. 2002, *A&A*, 387, 1066
- Bulanov, S. V., & Sasorov, P. V. 1976, *Soviet Astron.*, 19, 464
- Burkhart, G. R., Drake, J. F., & Chen, J. 1991, *J. Geophys. Res.*, 96, 11539
- Camilo, F., Manchester, R. N., Gaensler, B. M., & Lorimer, D. R. 2002, *ApJ*, 579, L25
- Chatterjee, S., & Cordes, J. M. 2002, *ApJ*, 575, 407
- . 2004, *ApJ*, 600, L51
- Contopoulos, I., Kazanas, D., & Fendt, C. 1999, *ApJ*, 511, 351
- Cordes, J. M., Romani, R. W., & Lundgren, S. C. 1993, *Nature*, 362, 133
- Coroniti, F. V. 1990, *ApJ*, 349, 538
- Cowley, S. W. H. 1971, *Cosmic Electrodyn.*, 2, 90
- . 1973, *Cosmic Electrodyn.*, 3, 448
- Del Zanna, L., Amato, E., & Bucciantini, N. 2004, *A&A*, 421, 1063
- Demorest, P., Ramachandran, R., Backer, D. C., Ransom, S. M., Kaspi, V., Arons, J., & Spitkovsky, A. 2004, *ApJ*, 615, L137
- Dessler, A. J. 1968, *J. Geophys. Res.*, 73, 209
- . 1971, *J. Geophys. Res.*, 76, 3174
- Gaensler, B. M., Fogel, J. K. J., Slane, P. O., Miller, J. M., Wijnands, R., Eikenberry, S. S., & Lewin, W. H. G. 2003, *ApJ*, 594, L35
- Gaensler, B. M., Van der Swaluw, E., Camilo, F., Kaspi, V. M., Baganoff, F. K., Yusef-Zadeh, F., & Manchester, R. N. 2004, *ApJ*, 616, 383
- Goldreich, P., & Julian, W. H. 1969, *ApJ*, 157, 869 (GJ69)
- Gotthelf, E. V. 2001, in *AIP Conf. Proc. 586, Relativistic Astrophysics: 20th Texas Symp.*, ed. J. C. Wheeler & H. Martel (New York: AIP), 513
- Gruzinov, A. 2005, *Phys. Rev. Lett.*, 94, 021101
- Helfand, D. J., Gotthelf, E. V., & Halpern, J. P. 2001, *ApJ*, 556, 380
- Jones, D. H., Stappers, B. W., & Gaensler, B. M. 2002, *A&A*, 389, L1
- Kaspi, V. M., Ransom, S. M., Backer, D. C., Ramachandran, R., Demorest, P., Arons, J., & Spitkovsky, A. 2004, *ApJ*, 613, L137
- Kirk, J. G., & Lyubarsky, Y. 2001, *Publ. Astron. Soc. Australia*, 18, 415
- Komissarov, S. S., & Lyubarsky, Y. E. 2004, *MNRAS*, 349, 779
- Kulkarni, S. R., & Hester, J. J. 1988, *Nature*, 335, 801
- Lai, D., Chernoff, D. F., & Cordes, J. M. 2001, *ApJ*, 549, 1111
- Larrabee, D. A., Lovelace, R. V. E., & Romanova, M. M. 2003, *ApJ*, 586, 72
- Linde, T. J., Gombosi, T. I., Roe, P. L., Powell, K. J., & DeZeeuw, D. L. 1998, *J. Geophys. Res.*, 103, 1889
- Lovelace, R. V. E., Gandhi, P. R., & Romanova, M. M. 2005, *Ap&SS*, 298, 115
- Lovelace, R. V. E., & Romanova, M. M. 2003, *ApJ*, 596, L159
- Lyubarsky, Y., & Kirk, J. G. 2001, *ApJ*, 547, 437
- Ng, C.-Y., & Romani, R. W. 2004, *ApJ*, 601, 479
- Opher, M., et al. 2004, *ApJ*, 611, 575
- Pavlov, G. G., Kargaltsev, O. Y., Sanwal, D., & Garmire, G. P. 2001, *ApJ*, 554, L189
- Romani, R. W., Cordes, J. M., & Yadigaroglu, I.-A. 1997, *ApJ*, 484, 137L
- Romanova, M. M., & Lovelace, R. V. E. 1992, *A&A*, 262, 26
- Romanova, M. M., Toropina, O. D., Toropin, Yu. M., & Lovelace, R. V. E. 2001, in *AIP Conf. Proc. 586, Relativistic Astrophysics: 20th Texas Symp.*, ed. J. C. Wheeler & H. Martel (New York: AIP), 519
- . 2003, *ApJ*, 588, 400
- Schvartsman, V. F. 1970, *Soviet Astron.*, 14, 527
- . 1971, *Soviet Astron.*, 15, 377
- Speiser, T. W. 1970, *Planet. Space Sci.*, 18, 613
- Spitkovsky, A., & Arons, J. 2004a, *AAS HEAD Meeting 8*, 8.02
- . 2004b, *ApJ*, 603, 669
- Spruit, H., & Phinney, E. S. 1998, *Nature*, 393, 139
- Stappers, B. W., Gaensler, B. M., Kaspi, V. M., van der Klis, V., & Lewin, W. H. G. 2003, *Science*, 299, 1372
- Thorsett, S. E., Briskin, W. F., & Goss, W. M. 2002, *ApJ*, 573, L111
- Toropina, O. D., Romanova, M. M., Toropin, Yu. M., & Lovelace, R. V. E. 2001, *ApJ*, 561, 964
- Treves, A., & Colpi, M. 1991, *A&A*, 241, 107
- van der Swaluw, E., Achterberg, A., Gallant, Y. A., Downes, T. P., & Keppens, R. 2003, *A&A*, 397, 913
- van Kerkwijk, M. H., & Kulkarni, S. R. 2001a, *A&A*, 378, 986
- . 2001b, *A&A*, 380, 221
- Vasyliunas, V. M. 1980, *J. Geophys. Res.*, 85, 4616
- Vlahakis, N. 2004, *ApJ*, 600, 324
- Walter, F. M. 2001, *ApJ*, 549, 433
- Weisskopf, M. C., et al. 2000, *ApJ*, 536, L81
- Wilkin, F. P. 1996, *ApJ*, 459, L31
- Yusef-Zadeh, F., & Bally, J. 1987, *Nature*, 330, 455
- Zank, G. P. 1999, *Space Sci. Rev.*, 89, 413
- Zenitani, S., & Hoshino, M. 2001, *ApJ*, 562, L63